SIMPLE CALCULATION OF GEOMETRICAL SHIELDING AT INTERGRANULAR CRACK FRONT BY MEANS OF PYRAMIDAL MODEL

P. Šandera, J. Horníková and J. Pokluda

Brno University of Technology, Faculty of Mechanical Engineering, Technická 2, CZ-61669 Brno, Czech Republic

ABSTRACT: *The paper presents a simple pyramidal model of a real intergranular crack front enabling the analytical calculation of the effective stress intensity factor. This analytical approach yields values well comparable with the data obtained by a boundary element numerical procedure applied to real-like intergranular crack fronts. It enables to separate the geometrical shielding level from the measured fracture toughness values in order to obtain the real averaged grain boundary fracture energy. In this way, some apparently paradox phenomena can be quantitatively elucidated, e.g. the increase in fracture toughness with increasing solution annealing temperature in ultra-high strength low alloy steels.*

INTRODUCTION

The fracture toughness can be assumed to be composed of intrinsic and extrinsic (shielding) components [1]. In order to separate the shielding component at intergranular front, a calculation of the effective stress intensity factor for real-like fronts is to be performed using special numerical methods. The local mixed mode described by local stress intensity factors k_1, k_2, and k_3 acts at 3D crack fronts even in case of a pure remote mode I loading. The global normalised effective stress intensity factor can be expressed as

$$k_{effg}^2 = \frac{\frac{1}{B}\int_0^B k_{eff}^2 \, \mathrm{d}z}{R_S}, \qquad (1)$$

where B is the specimen thickness, z is the Cartesian co-ordinate along the thickness, R_S is the surface roughness, $k_{eff}^2 = k_1^2 + k_2^2 + (1-\nu)^{-1} k_3^2$ and ν is the Poisson's ratio [2].

The main aim of this paper is to present a simple pyramidal model of the intergranular crack front enabling to asses the global effective stress intensity factor. Conditions of both the small-scale yielding and plane strain are assumed to be particularly fulfilled in this analysis. Together with the statistical theory based on the size ratio effect, the model is applied to quantitative elucidation of the antagonistic behaviour of fracture toughness and absorbed energy in the ultra-high strength steel P-LDHA.

PYRAMIDAL MODEL

The intergranular subcritical crack can be simulated by a narrow tortuous band following the grain boundary network in the related 3D Voronoi tessellation (see Figure 1). The k_{effg} -factor for this front corresponds well to a simple periodic pyramid-like geometry [3] – see Figure 2. Each oblique segment of the pyramidal geometry represents one grain of the regular grain boundary network of the mean grain size d_m. The value $\Phi = \pi/4$ with respect to the macroscopic crack plane corresponds to the linear roughness R_L = 1,41 ($R_S \approx 1.6$) typical for intergranular crack surfaces [4]. The angles Θ_m and Φ are related as

$$d_m . \tan\Phi = r_p . \tan\Theta_m , \tag{2}$$

$$r_p \approx \frac{1}{2\pi}\left(\frac{K_{Ic}}{\sigma_y}\right)^2 , \tag{3}$$

where r_p is the plastic zone size at the unstable fracture initiation, K_{Ic} is the fracture toughness and σ_y is the yield stress.

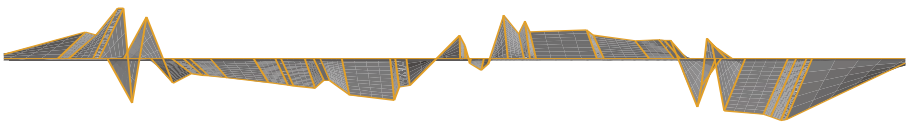

Figure 1: Computer model of the intergranular crack front based on 3D Voronoi tessellation.

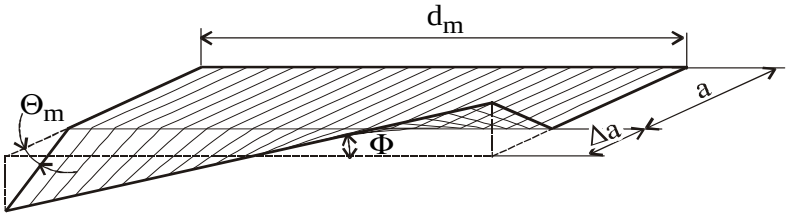

Figure 2: Element of the pyramidal approximation of the intergranular crack front band.

In the fracture toughness test, the stable intergranular crack develops within the process zone of a size Δa proportional to that of the plastic zone of the *a priori* crack. The one half of the plastic zone size r_p can be accepted as a plausible measure of Δa, i.e. $\Delta a = r_p / 2$. The factor k_{effg} can be calculated by using approximate analytical expressions for local stress intensity factors (normalised to the remote K_I factor)

$$
\begin{aligned}
k_1 &= \cos^6\left(\frac{\Theta}{2}\right).\left[2\nu\sin^2\Phi + \cos^2\left(\frac{\Theta}{2}\right)\cos^2\Phi\right] + \\
&\quad + \sin^2\left(\frac{\Theta}{2}\right)\cos^4\left(\frac{\Theta}{2}\right)\left[2\nu\sin^2\Phi + 3\cos^2\left(\frac{\Theta}{2}\right)\cos^2\Phi\right], \\
k_2 &= \sin\left(\frac{\Theta}{2}\right)\cos^2\left(\frac{\Theta}{2}\right), \\
k_3 &= \cos^6\left(\frac{\Theta}{2}\right).\sin\Phi\cos\Phi\left[\cos^2\left(\frac{\Theta}{2}\right) - 2\nu\right] + \\
&\quad + \sin^2\left(\frac{\Theta}{2}\right)\cos^4\left(\frac{\Theta}{2}\right)\sin\Phi\cos\Phi\left[3\cos^2\left(\frac{\Theta}{2}\right) - 2\nu\right].
\end{aligned}
\tag{4}
$$

Eq. 4 holds reasonably well for $\Delta a \ll a$ (a is the length of an *a priori* fatigue crack). By using the pyramidal model, Eq. 1 can be written as

$$
k_{effg}^2 = \frac{1}{3.2\Theta_m}\int_{-\Theta_m}^{\Theta_m}\left(k_1^2 + k_2^2 + \frac{k_3^2}{1-\nu}\right)\mathrm{d}\Theta. \tag{5}
$$

Application of the FRANC3D numerical code has shown that substitution of Eq. 4 to Eq. 5 yields k_{effg} values very close to those for real-like intergranular surfaces in a sufficiently wide range of R_S [3,4].

GEOMETRICAL SHIELDING AT INTER-TRANSGRANULAR CRACK FRONT

Values of fracture toughness and impact-absorbed energy of steels are usually well correlated [5]. The pyramidal model can be applied to the elucidation of the inverse relation between fracture toughness and impact absorbed energy values found in the ultra-high strength low alloyed steel P-LDHA (AISI 4340 steel with an increased Si content) [6]. Various heat treatments according to Table 1 resulted, in all cases, in the martensitic matrix type with different mean values of the prior austenite grain size. The standard heat treatment S1 – 870^0C solution annealing and 300^0C tempering – gives optimal tensile and fatigue mechanical properties. The yield strength of all specimens was nearly the same ($\sigma_y = 1500$ MPa) as determined by the martensitic matrix.

TABLE 1. Heat treatment and mean prior austenite grain size

Solution annealing and quenching	Tempering	Symbol	Grain size [μm]
870°C/1 h/oil	300°C/2h/air	S1	25
1050°C/1,5 h/oil	300°C/2h/air	S2	70
1200°C/1,5 h/oil	300°C/2h/air	S3	120

Specimens were subjected to the standard fracture toughness test K_{Ic} using three-point bend specimens (FT specimens). Charpy V-notch and U-notch (2 mm radius) impact toughness tests (CVN and UN specimens) were made as well. Results of mechanical tests are shown in Figure 3. As can be clearly seen, the fracture toughness curve K_{Ic} vs. d is completely inverse to both the CVN- and UN absorbed energy.

Fracture morphology of fine-grained (25 μm) FT specimens was transgranular ductile with a very flat surface, those of 75 μm exhibited a mixed inter-trans morphology ($\approx 75\%$ intergranular) whereas coarse-grained samples were intergranular (along prior austenite grain boundaries).

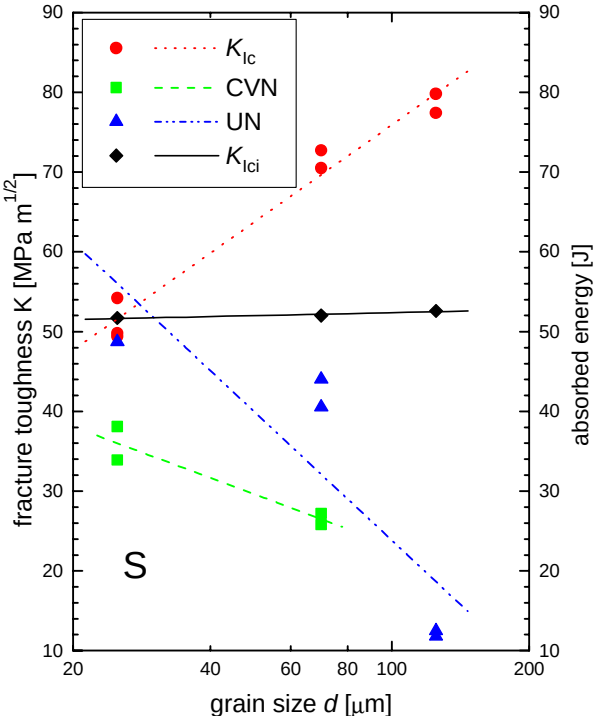

Figure 3: Dependence of fracture toughness and absorbed energy values on the mean austenite grain size for S-specimens.

Fracture surface morphology near the notch differed substantially when comparing the fine grained and coarse-grained UN or CVN samples. A wide shear zone adjacent to the notch surface was clearly distinguishable in case of the fine-grained structure S1. On the other hand, the shear zone of the coarse-grained structure S3 was very narrow and worse distinguishable. Details of the fracture morphology of all the FT and UN samples are presented elsewhere [6].

The probability of appearance of the intergranular morphology can be theoretically estimated using the statistical concept of the roughness-induced shielding [2]. This approach is based on the so-called size ratio effect, i.e. on the ratio $S_R = d / r_p$, where d is the characteristic microstructure distance. Microstructure elements are divided into two main categories - with a low S_R ($d \ll r_p$) and a high S_R ($d \geq r_p$). The low-S_R part of the probability density function $p(S_R)$ does not contribute to the shielding. The critical value S_{Rc} determining the boundary between both

types of the microstructure distance should lie within the range of $S_{Rc} \in (0.3, 3)$. Thus, the relative length of the crack front (or of the fracture surface profile) contributing to the shielding effects can be expressed as

$$\eta = \frac{\int_{S_{Rc}}^{\infty} S_R . p(S_R) \mathrm{d}S_R}{\int_0^{\infty} S_R . p(S_R) \mathrm{d}S_R} . \tag{6}$$

For a particular material, the value η can be calculated when knowing both the statistical distribution of d (from the metallographical analysis) and the yield stress σ_y in order to estimate the plastic zone size. The two-parameter (μ, ξ) Weibull probability density function

$$p(S_R) = \frac{\xi S_R^{\xi-1}}{\mu^{\xi}} \exp\left[-\left(\frac{S_R}{\mu} \right)^{\xi} \right] \tag{7}$$

is to be used. Then the mean size ratio can be expressed as

$$S_{Rm} = \frac{d_m}{r_p} = \mu \Gamma\left(1 + \frac{1}{\xi} \right), \tag{8}$$

where d_m is the mean characteristic microstructure distance and Γ is the Gamma function. For commercial steels, the value $\xi = 2.2$ can be accepted as a typical average [7]. Hence, using the plausible value $S_{Rc} = 0.5$, the parameter η can be plotted as a function of the mean austenite grain size d_m - see Figure 4. This function reproduces very well the fraction of intergranular morphology of samples with different mean grain size.
Applying a simple proportional rule, the case of a general mixed inter-transgranular shielding can be described as

$$k_{effg}^{mix} = 1 - \eta + \eta k_{effg} \tag{9}$$

since the straight transgranular facets do not contribute to the shielding effect ($k_{eff} = 1$, $R_S = 1$). Values k_{effg}^{mix} calculated according to Eqs. $5-9$ and multiplied by measured K_{Ic} values, i.e. the intrinsic K_{Ici} values, are plotted in Figure 3. The K_{Ici} values of all specimens are well comparable. However, a partial splitting (forking) of the crack front can also accompany

the intergranular fracture. This phenomenon, which was not included into the calculation procedure, can cause an additionally shift of the intrinsic level towards lower values for coarse-grained samples. In spite of this possible slight shift, the resistance of grain boundaries to the crack propagation does not seem to be much lower than that of the grain interior.

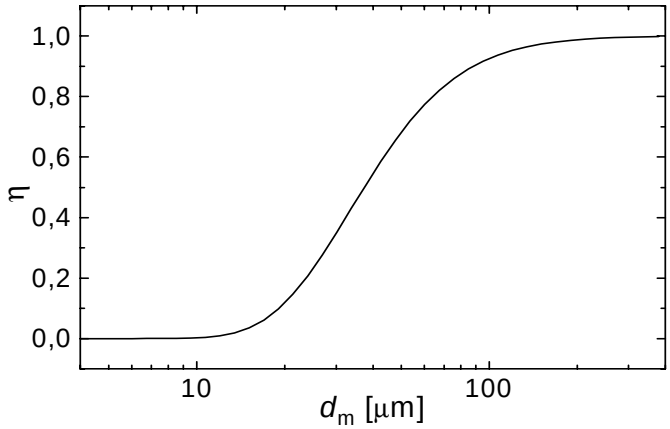

Figure 4: Theoretical fraction of intergranular morphology in dependence on the mean austenite grain size.

In the CVN- and UN specimens, unlike in FT specimens, the crack must first nucleate within the plastic zone in the bulk and, after linking with the notch surface by shearing, it propagates further in an unstable manner. Both the high concentration of carbides and larger dislocation pile-ups at grain boundaries produce a network of microcracks within the notch plastic zone of coarse grain structures. One of those intergranular crack nuclei (sufficiently near to the free surface) initiates an easier linking process and subsequent unstable intergranular growth following the microcrack network. The shear zone near the notch is very narrow and the work needed for crack initiation is small. In fine-grained structures, however, the crack initiates within a rather homogeneous plastic zone in the bulk in a relatively high distance from the free notch surface (site of a highest stress triaxiality). The linking process is accompanied by a large-scale plastic strain. Consequently, the shear zone is wide and the related crack initiation work is high. Hence, the absorbed energy decreases in contradiction to the fracture toughness K_{Ic}.

CONCLUSION

The simple pyramidal model of the real-like intergranular crack front yields values of the global effective stress intensity factor well comparable with the real-like data computed by numerical procedures. This model was used for a quantitative elucidation of the inverse relation between the fracture toughness and absorbed energy found in the ultra-high strength low alloy steel. After reduction of measured fracture toughness values by the geometrical shielding, the intrinsic values of all steel grades become close to the value of 52 $MPam^{1/2}$ regardless of the prior austenite grain size. The drop in the absorbed energy can be understood in terms of a decreasing crack initiation work.

ACKNOWLEDGEMENT

This work was supported by the European agency COST (Action 517) and by the Ministry of Education and Youth of the Czech Republic under the Grant No. OC 517.30 (1998).

REFERENCES

1. Ritchie R.O. (1988) *Mat. Sci. Eng.* **A103**, 15.
2. Pokluda J. (2001) *Mechanika* **67**, 277.
3. Šandera P., Pokluda J., Horníková J. (2001). In: *Material Structure & Micromechanics of Fracture (MSMF-3)*, pp.786-790, Šandera, P. (Ed.). Vutium, Brno University of Technology.
4. Pokluda J., Saxl I., Šandera P., Ponížil P., Matoušek M., Podrábský T., Horníková J. (2000). In: *Advances in Mechanical Behaviour, Plasticity and Damage - Euromat 2000*, pp.449-453, Miannay, D., Costa, P., Francois, D., Pineau, A. (Eds.). ELSEVIER.
5. Server W.L. (1992). In: *ASM Handbook, Vol. 8, Mechanical Testing*, pp.261-268, Newby, J.R. et al. (Eds.). ASM International.
6. Pokluda J., Vlach B., Šandera P., Jurášek L. (2001). In*: Cleaner Metal for Industrial Exploitation*, pp.126-133, Lecomte-Beckers, J. et al. (Eds.). Office for Official Publications of the European Communities, Luxembourg.
7. Pokluda J., Šandera P., Horníková J. (2000). In: *Fracture mechanics: applications and challenges, ECF 13*. CD-ROM. Fuentes, M. et al. (Eds.). ELSEVIER.